UNIVERSITY OF CALIFORNIA,
IRVINE

# Porous Media Flow Field for Proton Exchange Membrane Fuel Cells: Depression of Gas Diffusion Layer Intrusion and Delamination

THESIS

submitted in partial satisfaction of the requirements
for the degree of

MASTER OF SCIENCE

in Mechanical and Aerospace Engineering

by

Bo Zheng

Thesis Committee:
Professor Yun Wang, Chair
Professor Feng Liu
Assistant Professor Jaeho Lee

2019

# TABLE OF CONTENTS

# LIST OF FIGURES

# LIST OF TABLES

# ACKNOWLEDGMENTS

I would like to express the deepest appreciation to my committee chair, Professor Yun Wang, who inspires me to focus on fuel cell research area. Not only did he give me crucial suggestions every time when I have troubles, but he offered me chances to help me go father in my research. I would like to appreciate the advice from my committee members, Professor Feng Liu and Jaeho Lee, who help me in comprehending the underlying principles which helped me to construct the models in this thesis.

Additionally, I would also like to thank my parents and my wife, they spent most of time to take care of my daughter. So that, I can have enough time to finish my thesis. Moreover, I would like to thank my daughter, Hannah Zheng, who brings so much happiness to my family.

# ABSTRACT OF THE THESIS

Porous Media Flow Field for Proton Exchange Membrane Fuel Cells: Depression of Gas Diffusion Layer Intrusion and Delamination

By

Bo Zheng

Master of Science in Mechanical and Aerospace Engineering

University of California, Irvine, 2019

Professor Yun Wang, Chair

GDL is an important component of Proton Exchange Membrane Fuel Cell, which provides multi-functions： reactant transport, heat/water removal, mechanical support to the membrane electrode assembly (MEA), and protection of the catalyst layer from corrosion or erosion. GDLs are located between MPLs and bipolar plates, and gases reactants are distributed in the flow field channels and diffuses to the catalyst layer via GDLs. This study is to investigate the deformation or intrusion of GDL upon compression, which alters the channel cross-section and hence the flow conductance for PEM fuel cells. A 3-dimensional finite element model by ANSYS was developed to simulate the GDL deformation under various compression. Deformation or intrusion of GDL will reduce the space of gas flow channel and thus affect the performance of PEM fuel cell. As the compression pressure increases, the GDL intrusion area into the channel increases. The intrusion also increases with the increasing of width of the channel under the same pressure if the GDL-MPL interface is fixed. In addition, if the height of GDL increases, the intrusion of GDL into the channel also increases. When the GDL is 0.2 mm, channel width is 2mm, the pressure is 1

MPa, the intrusion of GDL is 0.05749 mm. When the GDL is 0.3 mm, channel width is 2mm, the pressure is 1 MPa, the intrusion of GDL is 0.08314 mm. To investigate the GDL-MPL interfacial force, the MPL is added to be in touch with the GDL. The simulation shows that the force will change with the increasing pressure. That means they may separate when the pressure increases to a point. In this study, the effect of porous media to the deformation of GDL and the delamination between GDL and MPL are studied. It was investigated in comparison with the traditional hollow channel configuration. Porous media flow field was first proposed by Wang in 2008, which uses porous materials such as metal foams and carbon felts in the channel space and utilizes the multi-functions of porous materials for heat, electron, and flow conductance. It is found that this new porous media flow field reduces the intrusion of GDLs under land compression with reduction dependent on the channel depth and Young's modulus of the porous material. For a channel depth of 0.3 mm and Young's modulus of 6.3 MPa, the intrusion was reduced by 21.1%. In addition, the tensile force between GDL and MPL is also depressed by introducing the porous media flow field. For the cases of channel full of porous media, only compressive stress was predicted, which avoids any separation or delamination between the GDL and MPL. The impact on the interfacial force is found to be a function of the channel width, Young's modulus of the porous material, and land compression. The findings are important to design porous media flow field for PEM fuel cell applications.

# Chapter.1 INTRODUCTION

## 1.1 PEM Fuel Cell

Fuel cell [1] is a power generation device that mainly converts chemical energy in fuel into electrical energy. It has highly efficient and no mechanical transmission components, so there is no noise pollution and very few harmful gases are emitted. Fuel cells are considered as the most promising power generation technology from the perspective of energy conservation and ecological protection [2]. Among the different types of fuel cells, polymer electrolyte membrane fuel cells are considered the most potential due to their high efficiencies and almost zero emissions. PEM fuel cells are constructed using polymer electrolyte membranes (notably Nafion®) as proton conductor and Platinum (Pt)-based materials as catalyst. Their noteworthy features include low operating temperature, high power density, and easy scale-up, making PEM fuel cells a promising candidate as the next generation power sources for transportation, stationary, and portable applications [2].

A typical PEMFC consists of bipolar plates, gas channels, gas diffusion layers (GDLs), and a proton-conductive membrane with platinum catalyst coated on each side, called the membrane electrode assembly (MEA), as shown in Fig. 1.1 [3]. Gas channels are grooved in graphite or metal plates, where injected reactant streams are distributed for electrochemical reactions. Protons are produced from hydrogen oxidation in the anode catalyst layer, and pass through the membrane, carrying water molecules via electro-osmotic drag, to the cathode catalyst layer where the oxygen reduction reaction (ORR)occurs with water as byproduct [4].

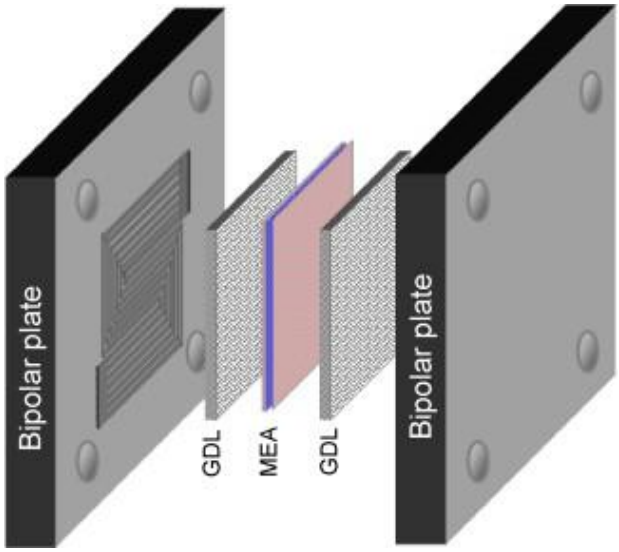


Figure 1.1. Main cell components

Micro-porous layer (MPL) is a porous layer located between the catalyst layer (CL) and gas diffusion layer (GDL). It is composed of carbon black powder and hydrophobic agent such as PTFE is applied on one side or two sides of the GDB, which is intended to provide a proper pore structure and wettability to allow effective gas and water transport and furthermore decrease the electric contact resistance between the GDL and the adjacent components [5].

The two plates on each side of the membrane electrode assembly is bipolar plate. The fully functioning bipolar plates are essential for multicell configurations by electrically connecting the anode of one cell to the cathode of the adjacent cell. The bipolar collector/separator plates have several functions in a fuel cell stack, such as, connect cells electrically in series, separate the gases in adjacent cells, provide structural support for the stack, conduct heat from active cells to the cooling cells or conduits typically house the flow field channels [6].

Fuel cell operating conditions include many ways [6]. First, pressure, A fuel cell may be operated at ambient pressure or it may be pressurized. As we have already learned, a fuel cell gains some potential when the operating pressure is increased thus generating more power. Second, temperature, the operating temperature of practical fuel cells, similarly to operating pressure, must be selected from the system perspective, taking into account not only the cell performance but also the system requirements, particularly the size and parasitic power requirements of the heat management subsystem. Third, flow rates of reactant gases, the reactants' flow rate at the inlet of a fuel cell must be equal to or higher than the rate at which those reactants are being consumed in the cell. Fourth, humidity of reactant gases, Because the membrane requires water to maintain protonic conductivity both reactant gases typically must be humidified before entering the cell. Fig. 1.2 is a fuel cell manufactured by PlugPower [1], Fig. 1.3 is schematic of a PEM fuel cell [1], and Typical PEM fuel cell operating conditions are listed in Table 1.1 [6].

Figure 1.2. A fuel cell manufactured by PlugPower

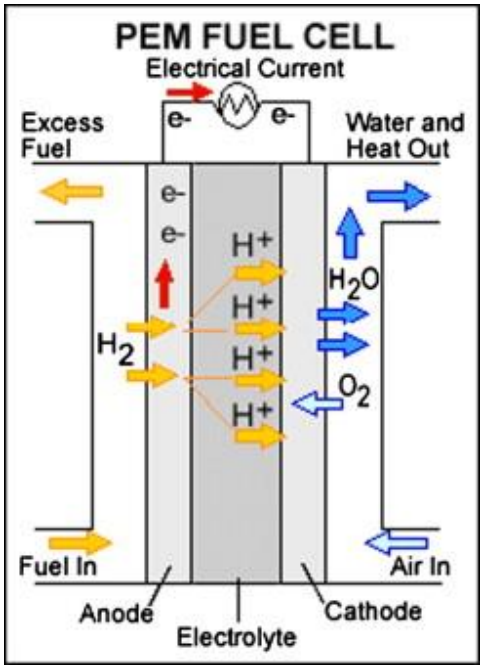


Figure 1.3. Schematic of a PEM fuel cell

Table 1.1. Typical Operating Conditions of PEM Fuel Cell

| | H2/air: Ambient to 400 kPa |
|---|---|
| Pressure | H2/O2: up to 1,200 kPa |
| Temperature | 50 °C to 80 °C |
| Flow rates | H2: 1 to 1.2 |
| | O2: 1.2 to 1.5 |
| | Air: 2 to 2.5 |
| Humidity of reactants | H2: 0 to 125% |
| | O2/Air: 0 to 100% |

## 1.2 GDLs and Gas Flow Channels

A layer between the catalyst layer and bipolar plates is called a gas diffusion layer, electrode substrate, or diffusor/current collector [6]. The GDLs, usually coated with micro-porous layers (MPLs), play an important role in electronic connection between the bipolar plate and the electrode and provide a passage for reactant transport and heat/water

removal. In addition, the GDL also performs the following essential functions: mechanical support to the membrane electrode assembly (MEA), and protection of the catalyst layer from corrosion or erosion caused by flows or other factors. A GDL typically consists of a macroporous substrate and a microporous layer (MPL) of carbon black [7]. Physical processes in GDLs, in addition to diffusive transport, include bypass flow induced by in-plane pressure difference between neighboring channels, through-plane flow induced by mass source/sink due to electrochemical reactions, heat transfer like the heat pipe effect, two-phase flow, and electron transport[3,4]. Niu [8] found that the effective diffusivity becomes lower under higher PTFE loading due to the decreased pore volume, as expected. Liquid water transport in perforated gas diffusion layers (GDLs) is numerically investigated using a three-dimensional (3D) two-phase volume of fluid (VOF) model and a stochastic reconstruction model of GDL microstructures. It is found that perforation can considerably reduce the liquid water level inside a GDL [9].

A three-dimension (3-D) model of polymer electrolyte fuel cells (PEFCs) is employed to investigate the complex, non-isothermal, two-phase flow in the gas diffusion layer (GDL). Phase change in gas flow channels is explained, and a simplified approach accounting for phase change is incorporated into the fuel cell model. It is found that the liquid water contours in the GDL are similar along flow channels when the channels are subject to two-phase flow [10]. Cho [11] found that for low liquid flow rates most model predictions show acceptable agreement with experimental data, while in the regime of high liquid flow rate only a few of them exhibit a good match. Correlation optimization is conducted for individual flow pattern. Wang [12] present an experimental study on measurement of the

thermal conductivity and heat pipe effect in both hydrophilic and hydrophobic (Toray TGP-H60) carbon papers (around 200 lm thickness) with/out liquid water. An experimental setup is developed for measuring thermal conductance at different liquid water contents and temperatures without dissembling the testing device for water addition. Wu [13] investigated the two-phase flow in a thin gas flow channel of PEM fuel cells and wall contact angle's impact using the volume of fluid (VOF) method with tracked two-phase interface. The VOF results are compared with experimental data, theoretical solution and analytical data in terms of flow pattern, pressure drop and water fraction. Lewis [14][15] demonstrated that consistent behavior in the change of the two-phase pressure when comparing different wettabilities arises with careful consideration of the experimental parameters to classify experiments of adiabatic two-phase flow in a single microchannel into three categories: homogeneous, hydrophobic mixed-wettability, and superhydrophobic mixed-wettability microchannels, in addition, they found that the applicability for the two-fluid model to predict both the two-phase pressure and the water film thickness in thin microchannels.

In fuel cells, the channel flow field are designed to provide an adequate amount of the reactants (hydrogen and oxygen) to the GDL and catalyst surface while minimizing pressure drop. The reactant channel of polymer electrolyte fuel cells PEFCs plays a crucial role in fuel cell operation. It supplies the gaseous reactants and removes product water for fuel cells [16]. The most popular channel configurations for PEM fuel cells are serpentine, parallel, and interdigitated flow. Recently, porous media was applied to the fuel cell channel region and allowing a simultaneous transport of the fluid flow through the

interconnected pores and heat/electrons via the solid matrix. This approach enhances the heat and electronic current transport in fuel cells and the flexibility of the channel design [16].

### 1.3 GDL Intrusion and Delamination

During the assembling process of a single cell or a stack, the membranes, bipolar plates and GDLs are clamped together by many bolts [17]. But, the pressure caused by the bolts after installation will result in deformation of GDL. At the same time, there will be some intrusion of GDL into gas channel, which will reduce the area of the channel. Gas diffusion layer (GDL) is one of the most important components which is usually made of porous carbon paper or carbon cloth, Figure 1.4 is their scanning electron microscope (SEM) micrographs [18]. GDL should adequate mechanical strength to protect the catalyst coated membrane.

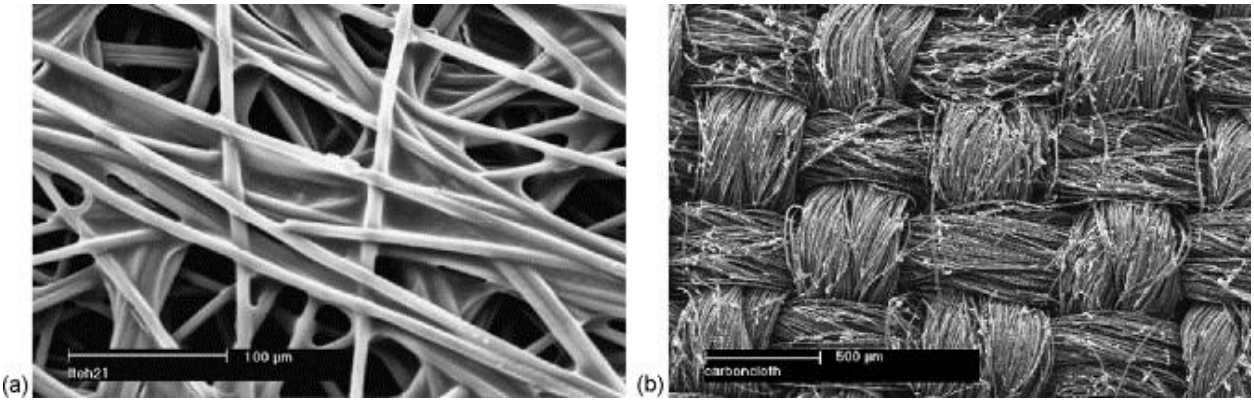


Figure 1.4. SEM micrographs of: (a) carbon paper and (b) carbon cloth.

Several theoretical and finite element analysis (FEA) models for predicting the deformation of GDL and interfacial contact resistance have been reported. An investigation is made of the effects of the change of the porosity of the gas diffuser layer (GDL) on the performance of a proton exchange
membrane (PEM) fuel cell [19]. Y.H. Lai [20] used a 2D finite element model to determine the intrusion of gas diffusion medium GDM into the channel, and they devised a test to verify the simulation results. X.lai [21] conducted a direct coupled mechanical-electrical FEM model for a real BP and GDL assembly to predict the contact resistance between them. Daniil Bogracheve [22] developed a linear elastic-plastic 2D model of fuel cell to analysis mechanical stress in MEA arising in cell assembly procedure, and they compared the simulation results with experiment data. They found that the experiment data were in a good agreement with numerical predictions.

A finite element analysis structural 3D model was built to simulate the cell stack assembly in S.H.LEE's study [23]. In the model, it contained all components and stacking sequence of the single cell. At the same time, they used a Fuji pre-scale pressure film replaced the MEA to test the pressure distribution. They found that the trends of the pressure distribution were very similar between the measurement and the simulation. I. Taymaz [24] also used a 3D model of the one single channel to simulate the deformation of GDL under different pressure. They found that the optimum assembly pressure occurred at between 0.5MPa and 1MPa. Under this condition, fuel cell had a highly efficient operating condition. Three numerical cases were conducted to investigate the effects of GDL deformation and intrusion on fuel cell operation by P.Chippar [25]. The results showed that the deformation

and intrusion can increase the degree of liquid saturation, membrane water content and current density distribution. Alex Bates et al. [26] successfully simulated 16-cell stack of fuel cell. They found that high stress regions located in the gasket between bipolar plate and MEA and GDL stress plot revealed good contact between BP and GDL. The simulation result had a good correlation with experiment data. J.T. Wang [17] found that the GDL above the channels intrudes into the gas channels as an assembly pressure is applied and accordingly non-homogeneous thickness and porosity along the cell in the in-plane direction appear. Wang [4] also developed a structure–performance relationship for gas diffusion layers (GDLs) of polymer electrolyte fuel cells (PEFCs), and hence to explain the performance differences between carbon paper (CP) and carbon cloth (CC). Three-dimensional simulations, based on a two-phase model with GDL structural information taken into account, were carried out to explore the fundamentals behind experimentally observed performance differences of the two carbon substrates.

Some research focused on micro-scale to study the deformation of GDL. Totzke [27] present a synchrotron X-ray tomographic study on the morphology of carbon fiber-based gas diffusion layer (GDL) material under compression. Zhou [28] built a micro-scale model to predict contact resistance between BPP and GDL. In their study, classical statistical contact model was used to simulate the surface roughness of BPP and randomly distributed fibers were used to model the GDL. The modeling results showed good agreements with experiment data with less than 20% discrepancy. The compressed GDL microstructure by the finite element method (FEM) for assembly pressure simulation was developed by Zhou [29]. It showed that non-uniform deformation of the GDL microstructure along the

thickness direction would be caused by assembly pressure. In the other research they also found the intrusion of GDL into the channel under different compression ratio and compared them with experiment data from X-ray tomographic imaging [30]. Zhou [31] found that a larger fiber diameter or higher porosity contributes to the water transport due to larger average pore size.

In experiment, some study reported deformation and intrusion of GDLs. Lee [32] found that changes in the performance of a PEM fuel cell are presented as a function of the compression pressure resulting from torque on the bolts that clamp the fuel cell. Ge [33] built a unique fuel cell test fixture was designed and created such that, without disassembling the fuel cell, varying the compression of the GDL can be achieved both precisely and uniformly. Besides, the compression can be precisely measured and easily read out. Using this special fuel cell fixture, the effects of GDL compression on PEM fuel cell performance under various anode and cathode flow rates were studied. they noted that there should be an optimal compression ratio at which the performance of the cell was maximized. So that, they suggested that GDL compression should be precisely controlled. In SG. Kandlikar's [34] study, they observed that the intrusion increased with increasing compression which was the same as expected. In addition, the uneven distribution of GDL intrusion into the gas channels was considered the important findings. K.D. Baik [35] investigated the correlation between anisotropic bending stiffness of GDL and land/channel width ratio. Alex Bates et al. [26] tested the pressure by bursting microcapsules since when pressure was applied to the film it changes colors from white to red. It showed a good idea about the distribution and magnitude of pressure across the

GDLs in a 16-cell stack. Chang [36] found that the through-plane electrical resistance of the carbon paper itself is not significant.

Nitta [37] presented a study on the effect of inhomogeneous compression of gas diffusion layer (GDL) caused by the channel/rib structure of flow-field plate. The experimentally evaluated properties are GDL intrusion into the channel, gas permeability, in-plane and through-plane bulk electric conductivities, and contact resistances at interfaces as a function of compressed thickness of GDL. They used a dial indicator to measure the intrusion and found that the deformation of GDL remained almost the same regardless of the width of the channel. They built a flowchart of the effects of increasing compression in Figure 1.5 [37].

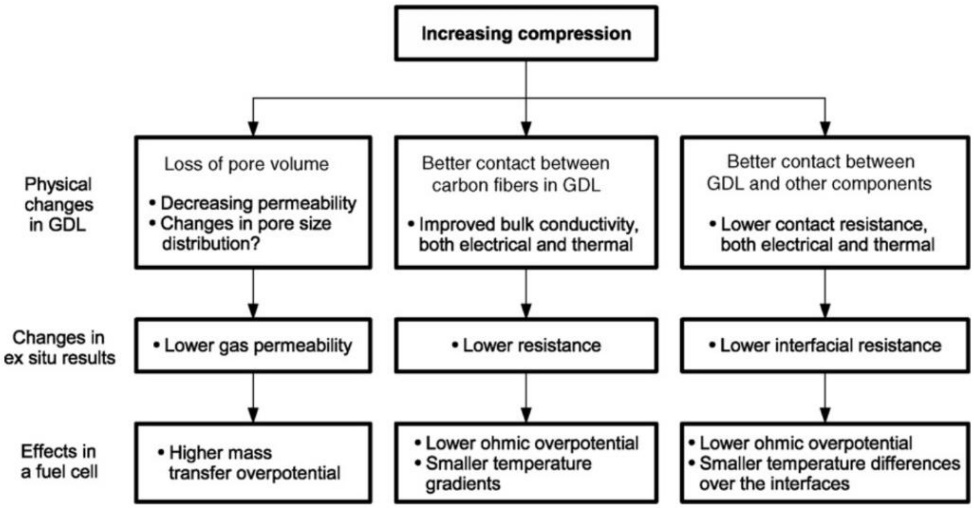


Figure 1.5. Effects of increasing compression over GDL

Porous media flow field has many benefits to PEMFC. Wang [3] theoretical analyses were performed and then built a three-dimensional model and develop numerical simulations to investigate the low humidity operation with both hollow and porous media channel. This

study showed that the porous media channels improved the characteristics of heat transport in the fuel cell. In addition, he developed a continuum model of two-phase channel flow which based on the M2 formalism to estimate the parameters key to fuel cell operation. The results showed that liquid water builds up quickly at the entrance region. Wang [2][3][16] proposed an approach of channel development for polymer electrolyte fuel cells which were fill porous media in the channel to improve reactant supply and byproduct removal. The porous media provided support over the diffusion media, thereby diminishing the concern of contact resistance under the channel. He dealt with the two-phase transport porous-media channel and found that the superficial gas velocity changes differently between single and two-phase regions and the proposed channel configuration results in a modest flooding for all considered cases. A novel metallic porous medium with improved thermal and electrical conductivities and controllable porosity was developed based on micro/nano technology for its potential application in PEM fuel cells [38]. Nguye [39] discussed measurements of two-phase transport properties of porous media. One was volume displacement technique, which could be sued to measure capillary properties of both hydrophilic and hydrophobic materials. The other was neutron imaging technique, which could be used to measure the capillary properties of thinner hydrophilic materials.

Sintered titanium powder and titanium foams of relative density ranging from 0.3 to 0.9 were produced by powder metallurgy routes and tested in uniaxial compression at low, medium and high rates of strain. At all strain rates, the foams deform by plastic collapse of the pores, accompanied by micro-cracking at compressive strains exceeding 0.2. The foams investigated are strain rate sensitive, with both the yield stress and the strain hardening

rate increasing with applied strain rate. The strain rate sensitivity is more pronounced for foams of lower relative density [40].

Some research focuses on the impact of interfacial delamination. In Kim's research [41], interfacial delamination between diffusion media and catalyst layers, but not between the catalyst layer and membrane, was observed. This permanent deformation of the stiff diffusion media in the channel locations as well as fractures of carbon fibers increased electrical resistance, and may increase water flooding, resulting in reduced longevity and operational losses. Later, he [42] built a two-dimensional anisotropic model to investigate the impact of local delamination on PEFC performance. Localized interfacial delamination of the membrane|catalyst layer and catalyst layer|diffusion media were found to increase ohmic resistance significantly. It showed that under frozen conditions, small interfacial delamination can result in a greater ohmic loss.

### 1.4 Objectives

This study is aimed at the impacts of porous media flow field on the GDL deformation under the channel and investigates the advantages of porous media flow field in enhancing fuel cell assembly and performance. For each type, four different pressure were considered and got the different intrusion. Under the same channel width, the intrusion increases with the increasing of pressure. This result shows the same as former study. Besides, one additional layer was studied in this research. It shows that with the pressure increases the force between GDL and additional layer changed from compressive stress to tensile stress.

That means they will separate with each other and there is a gap between them. To solve this problem, some porous media are put in the channel. They can reduce the intrusion of GDL and avoid the delamination between GDL and MPL or another layer. As a result, the performance of fuel cell will increase.

# Chapter.2 METHODS

The models developed in this study is the mechanical model by the finite element method in ANSYS. The mechanical model is developed for a three-dimensional (3D) domain composed of a single channel and the electrode of a PEM fuel cell. It is assumed that the components in both the cathode and the anode of the PEM fuel cell have the same structural change behavior, and accordingly, a half-cell domain is selected as the representative one, as shown in Figure 2.1. A mesh size of 2e-5 m was selected to create the elements, which was further refined at the upper and lower regions of the GDL interfaces. This mesh was validated by varying the mesh size in a range from 50% to 200% of the mesh size employed. The intrusion height varied only by less than 1.5%, which indicated that the 2e-5 m mesh size was appropriate [34].

## 2.1 Governing Equations

A three-dimensional domain compose of a single channel and a half cell domain is selected [17], as shown in Figure 2.1. The physical region modeled is located away from the edges of the PEMFC, consisting of the anode and cathode bipolar plate (BP), flow channel, GDL, and MPL. The assembly force on the top BP surfaces is considered uniformly distributed, and the influence caused by bending stress is neglected [43]. The Young's modulus for the GDL is much smaller than the BP, so for the cases without MPL, the assembly force mainly leads to the deformation of GDL. However, after adding MPL, the assembly force will cause the deformation of GDL and MPL. The present study considers the elastic deformation of the cell including the GDL and MPL, caused by assembly force, which is governed by the

equilibrium and compatibility equations with the Hooke's law serving as the constitutive relation [43].

$$\frac{\partial \sigma_i}{\partial x_i} + \frac{\partial \tau_{ij}}{\partial x_j} + \frac{\partial \tau_{ik}}{\partial x_k} + F_i = 0 \quad (1)$$

$$\frac{\partial^2 \varepsilon_i}{\partial x_j^2} + \frac{\partial^2 \varepsilon_j}{\partial x_i^2} - \frac{\partial^2 \gamma_{ij}}{\partial x_i \partial x_j} = 0 \text{ and } 2\frac{\partial^2 \varepsilon_i}{\partial x_j \partial x_k} = \frac{\partial}{\partial x_i}\left(-\frac{\partial \gamma_{jk}}{\partial x_i} + \frac{\partial \gamma_{ik}}{\partial x_j} + \frac{\partial \gamma_{ij}}{\partial x_k}\right) \quad (2)$$

$$\sigma_i = \lambda e + 2G\varepsilon_i \quad (3)$$

Where $\sigma_i$(Pa) is the normal stress, $\tau_{ij}$(Pa) the shear stress, $F_i$(Pa) the body force, $\varepsilon_i$ the normal strain, $\gamma_{ij}$ the shear strain, $\lambda$(Pa) the lame constant and G(Pa) the shear elastic modulus, and

$$\gamma_{ij} = \tau_{ij}/G, e = \varepsilon_i + \varepsilon_j + \varepsilon_k \quad (4)$$

$$\lambda = \frac{\mu E}{(1+\mu)(1-2\mu)} \quad (5)$$

$$G = \frac{E}{2(1+\mu)} \quad (6)$$

Where E(Pa) is the Young's modulus, and $\mu$ is the Poisson ratio. $i$, $j$ and $k$ represent the x, y, z coordinate, respectively.

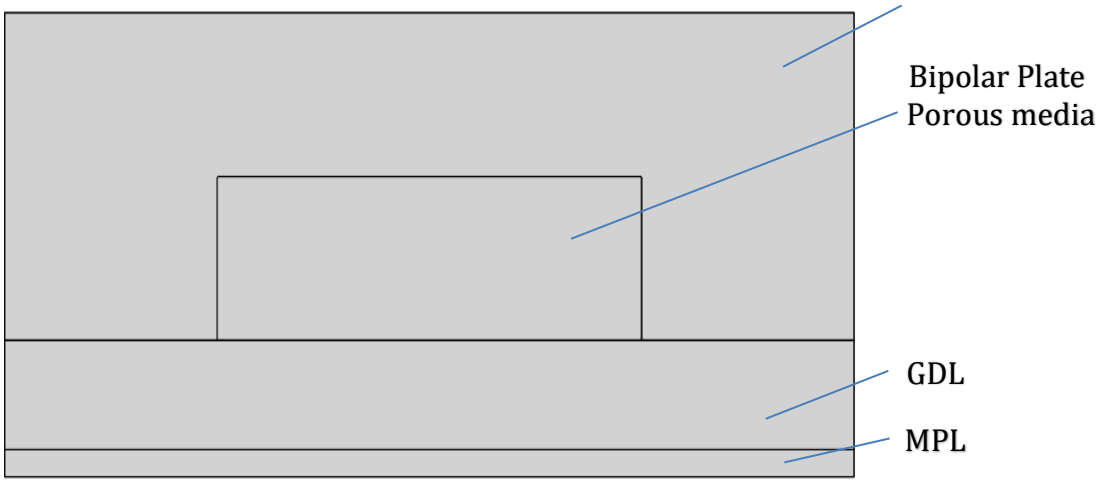


Figure 2.1. Geometry of the BP, porous media channel, GDL, and MPL.

## 2.2 Boundary Conditions

The bottom boundary surface was fixed, constraining all degrees of freedom to zero for no displace. The both side surfaces were applied displacement and X axis is 0, which means, there is no movement along X axis. All the layer interfaces are considered bonded so that they would not slip and rotate. The assembly pressure was applied on the top boundary surface of bipolar plates (in the through-plane direction in Figure 2.1) and a possible localized pressure distribution around the bolts is neglected. The pressure was positive, which means the pressure vertically point to the surface. After the loading was applied, the model was solved for a contour plot of the displacement due to compression and contacts pressure between the components of the cell were then determined. The outputs of the simulation were determined as the stress, strain, pressure distribution, and deformation of the fuel cell.

## 2.3 Numerical Implementation

The goal of this research was to propose a methodology and a FEA simulation procedure for establishing numerical tools for the evaluation of the stacking design and cell assembly parameters. From the numerical simulation, the methods of stacking design, the critical dimensions and material selection of fuel cell components, and assembly pressure were investigated for the purpose of achieving a consistent cell performance. The schematic plot of the methodology is shown in Figure 2.2 [23].

In this study, firstly, a fuel cell single channel model, which includes bipolar plate, GDL were designed for numerical simulation. After that, the models with porous media in channel and MPL were also considered. The compressive modulus of bipolar plate is much higher than the GDLs and MPL [44]. The bipolar plate is assumed as the structure steel in the simulation. The GDLs are the carbon papers which is a kind of fibers [45].

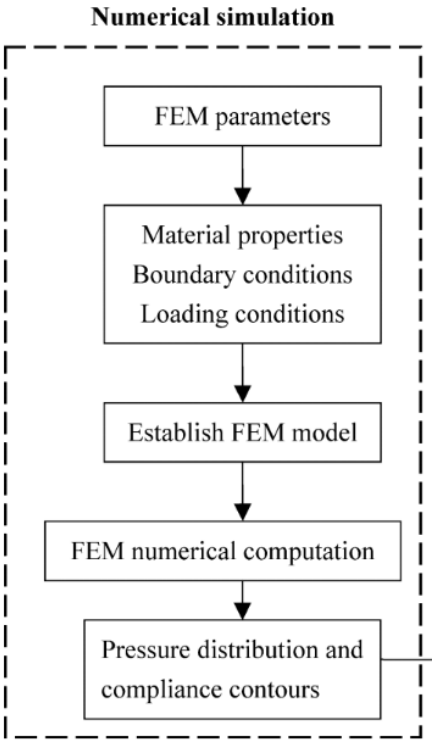


Figure 2.2. Schematic diagram of the simulation methodology.

ANSYS is used as the finite element method (FEM) software for the simulation. Different assembly pressure effects, ranging 0.5 MPa, 1 MPa, 1.5 MPa and 2 MPa, were tested by the program. The single cell deformation was calculated under these assembly pressures. For the FEA model, the mesh size is 2e-5m, as presented in figure 4. the width of the channel is 0.1mm. This model can well study the GDL and save the simulation time. The BP height is

0.9mm, total width of half single fuel cell is 2 mm, and four types of channel width were studied, 0.5mm, 0.75mm, 1mm, 1.5mm, corresponding to the channel/land width ratio are 0.67, 1.2, 2, 6. These four types of channel width contains most of types in market.

For the cases which the channel is full of porous media, we also consider the channel height, 0.3 mm, 0.6mm and 1mm. In addition, three different types of porous media are studied. One is the same as GDL's, one is 5 times of GDL's and the last one is 0.2 times of GDL's. According to the simulation results, the porous media will affect the deformation of GDL, and we can find a better material property to reduce the intrusion of GDL into the channel. We try to find good material of porous media which can help reduce the intrusion of GDL into the channel.

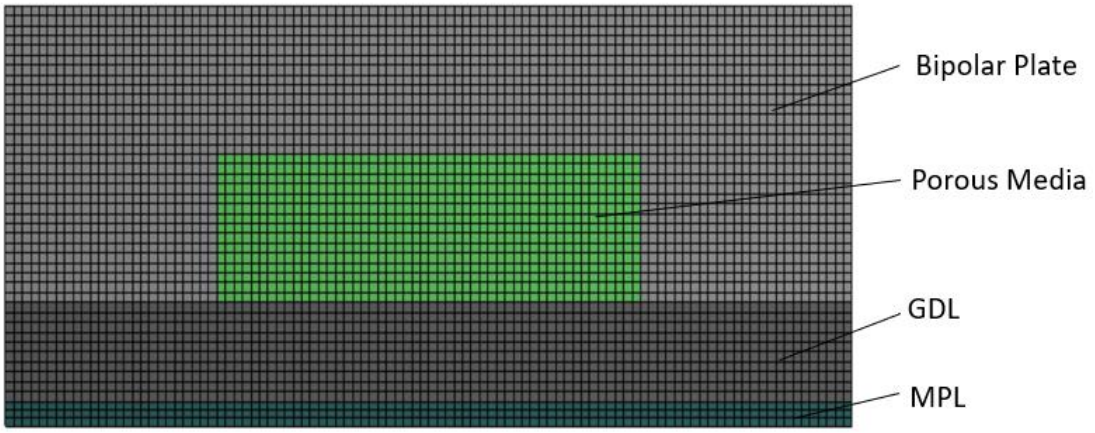


Figure 2.3. Computational domain

After that, MPL was considered to study the delamination between GDL and MPL. For the MPL's Young's modulus, we consider two types, one is the same as GDL's, the other is 5 times GDL's. Furthermore, we study the cases which the channel is full of porous media. This part, we focused on the contact pressure change between the GDL and MPL to predict

whether there is delamination between them or not. Geometrical and physical parameters of the model show in Table 2.1.

Table 2.1. Geometrical and physical parameters

| Parameter | Value |
|---|---|
| Channel height (mm) | 0.6 |
| BP height (mm) | 0.9 |
| BP width (mm) | 2 |
| BP Young's modulus (MPa) [26] | 21,000 |
| BP Poisson's ratio [26] | 0.28 |
| BP density (kg/m3) | 7,800 |
| GDL height (mm) | 0.2 |
| GDL width (mm) | 2 |
| GDL Young's modulus (MPa) [24] | 6.3 |
| GDL Poisson's ratio [24] | 0.09 |
| GDL density (kg/m3) | 400 |

# Chapter.3 RESULTS AND DISCUSSION

## 3.1 Comparation and general results

As the first step in the simulation study, one case was simulated according to one paper [20] to compare with their prediction results. Figure 3.1 is the present simulation result compared with the literature data. It shows that they almost the same.

During the assembly, the GDLs are clamped by BPs. In this simulation, we assume the GDL deformation in elastic zone. For hollow of channel cases, figure shows the stress distribution and deformation of GDL and BP when the pressure is 2 MPa, channel width is 1mm, channel height is 0.6 mm. Figure 3.2 a is the total Equivalent stress distribution of GDL and BP, b is the deformation of GDL and BP, c is Equivalent stress distribution of GDL, d is the deformation of GDL. Fig2 a and b show that there is intrusion of GDL into the channel, when a pressure is applied on the top surface of BP. Fig b also shows that GDL has a lager deformation than BP, because of BP's Young's modulus is much large than GDL's. Fig. c show that there is stress concentration in GDL, which will reduce the life of GDL. Some research added chamfer to avoid stress concentration [28], but they did know the best chamfer for GDL. For this part let's show more details and ways to solve this problem in next study.

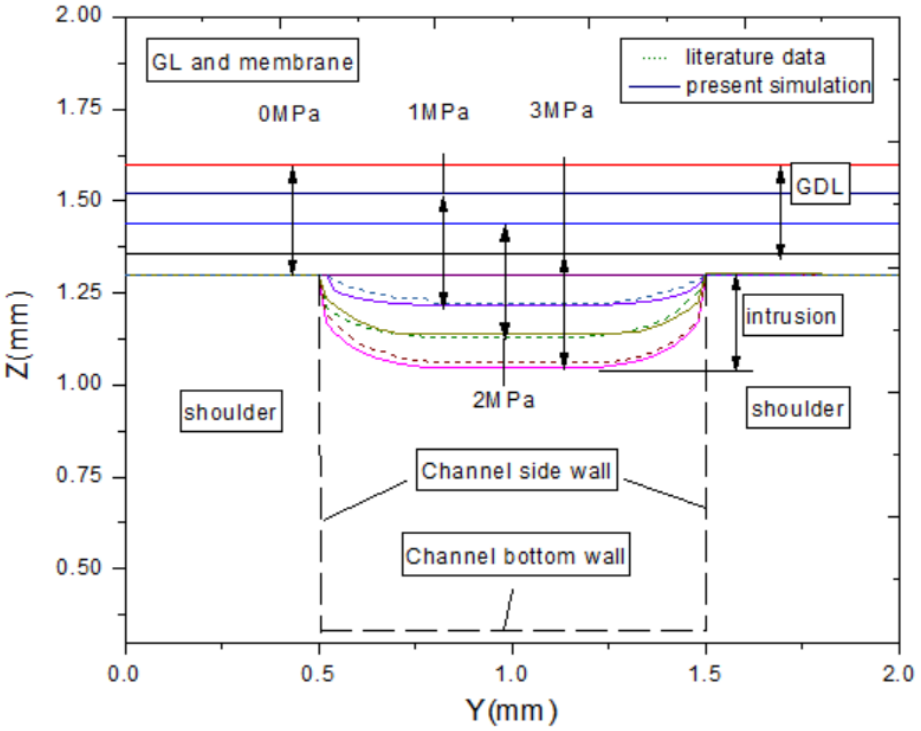


Figure 3.1. Comparison of simulation results with literature data.

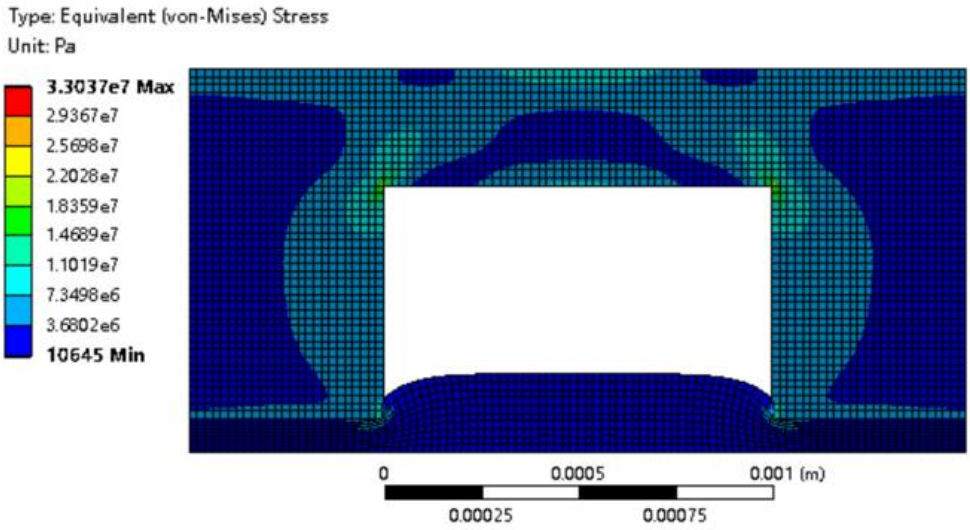


Figure 3.2a. Equivalent stress of BP and GDL

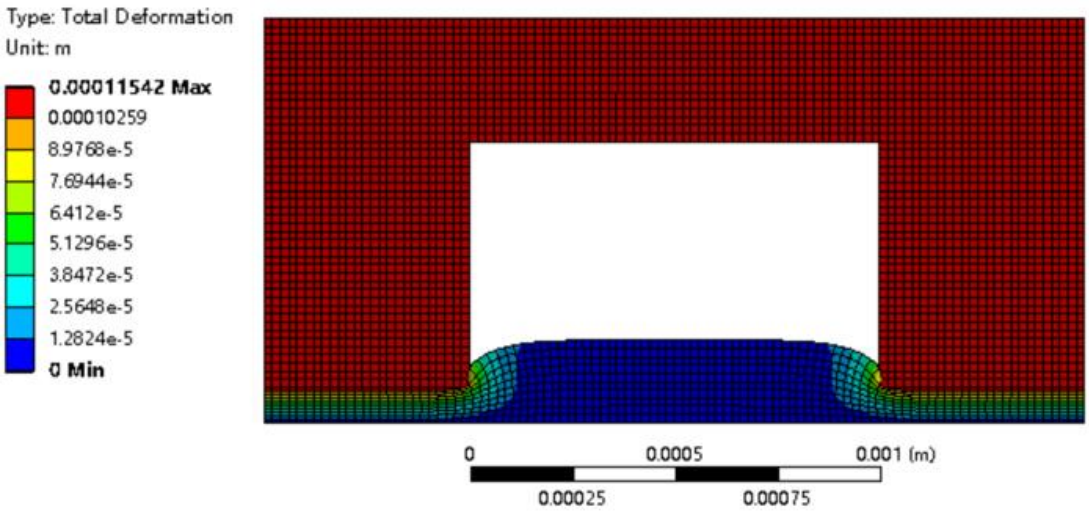


Figure 3.2b. Deformation of GDL under BP compression

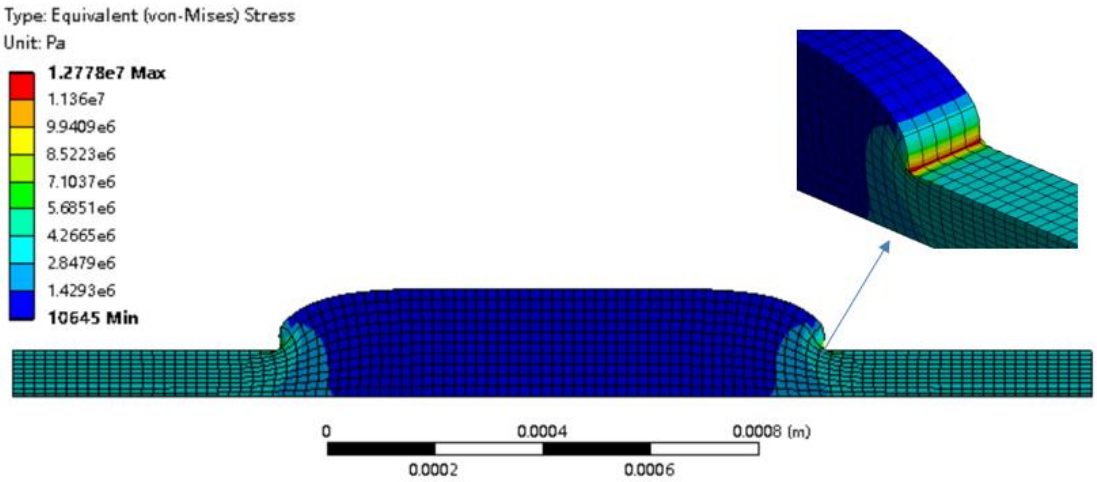


Figure 3.2c. Equivalent stress of GDL

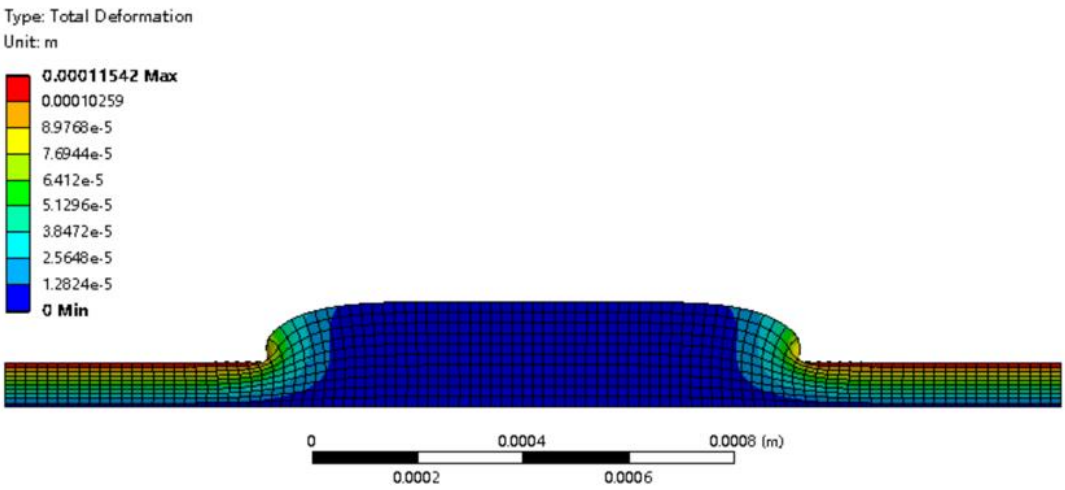


Figure 3.2d. Deformation of GDL under BP compression

Figure 3.2. a is the total Equivalent stress distribution of GDL and BP, b is the deformation of GDL and BP, c is Equivalent stress distribution of GDL, d is the deformation of GDL.

### 3.2 Effects of hollow channel on intrusion of GDL

When the channel is hollow, only BP and GDL are considered in this part. Figure 3.3 a, b, c and d show the shapes of the compression of GDL when the channel is 0.5, 0.75, 1.0, 1.5 mm under four different assembly pressures, that is 0.5, 1, 1.5, 2 MPa, respectively, and the height of GDL is 0.2 mm. The thickness of GDL is kept constant along the cell. Simulation results show that when the channel/land width ratio is the same, with the increasing of assembly pressure, the maximum of intrusion of GDL will increase. For example, Figure 3.3c shows that when the channel width is 1 mm, with the pressure change from 0.5 MPa to 2 MPa, the maximum of intrusion of GDL changes from 0.02874 mm to 0.11497 mm. for under each channel width, the trend is the same.

In addition, when the pressure is the same, if the channel/land width ration increasing, the maximum of intrusion of GDL also increases. Figure 3.4 shows that with the increase of channel width from 0.5 mm to 1.5 mm, the maximum of intrusion of GDL change from 0.03918 mm to 0.10591mm when the assembly pressure is 1 MPa. For under each assembly pressure, the trend is the same. The deformation of GDL when the channel width is 1.5 mm, pressure is 2 MPa is not considered since it is out of elastic zone.

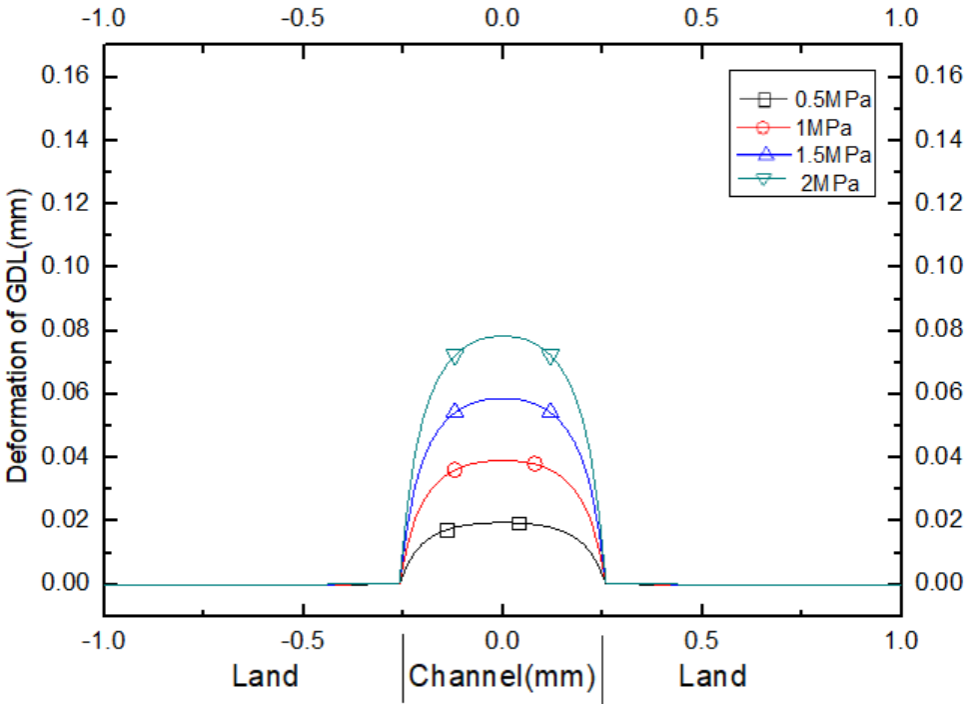


Figure 3.3a. Deformation of GDL for the channel width of 0.5 mm

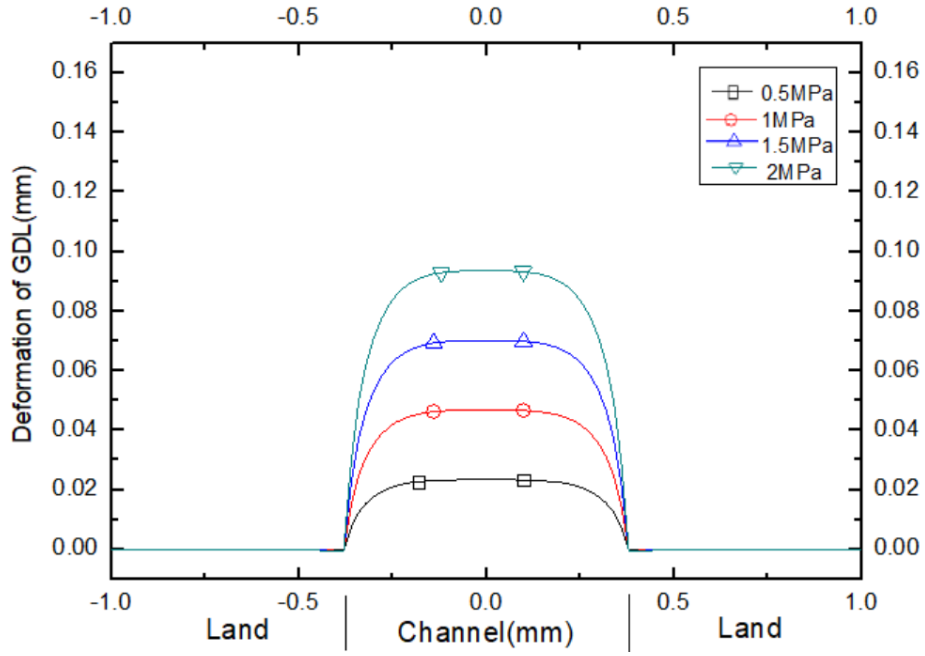


Figure 3.3b. Deformation of GDL for the channel width of 0.75 mm

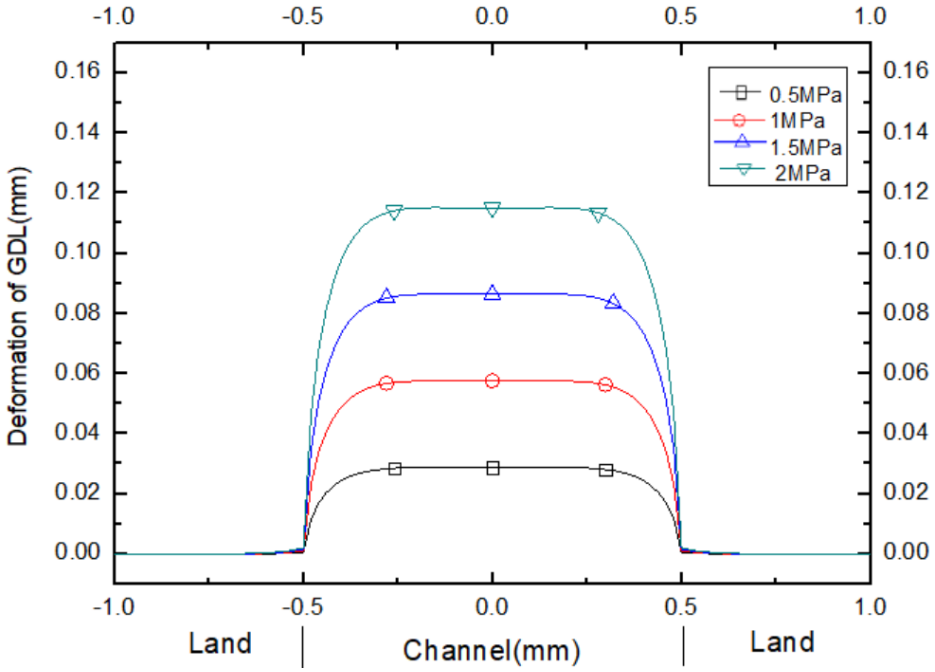


Figure 3.3c. Deformation of GDL for the channel width of 1 mm

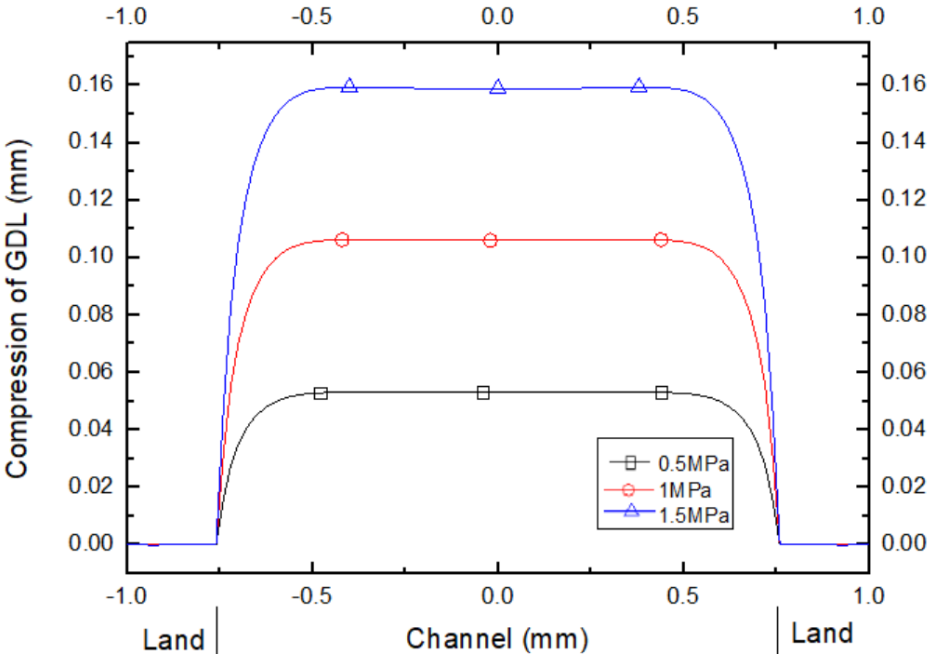


Figure 3.3d. Deformation of GDL for the channel width of 1.5 mm

Figure 3.3. a, b, c and d are the shapes of the compression of GDL when the channel is 0.5, 0.75, 1.0, 1.5 mm under four different assembly pressures, that is 0.5, 1, 1.5, 2 MPa.

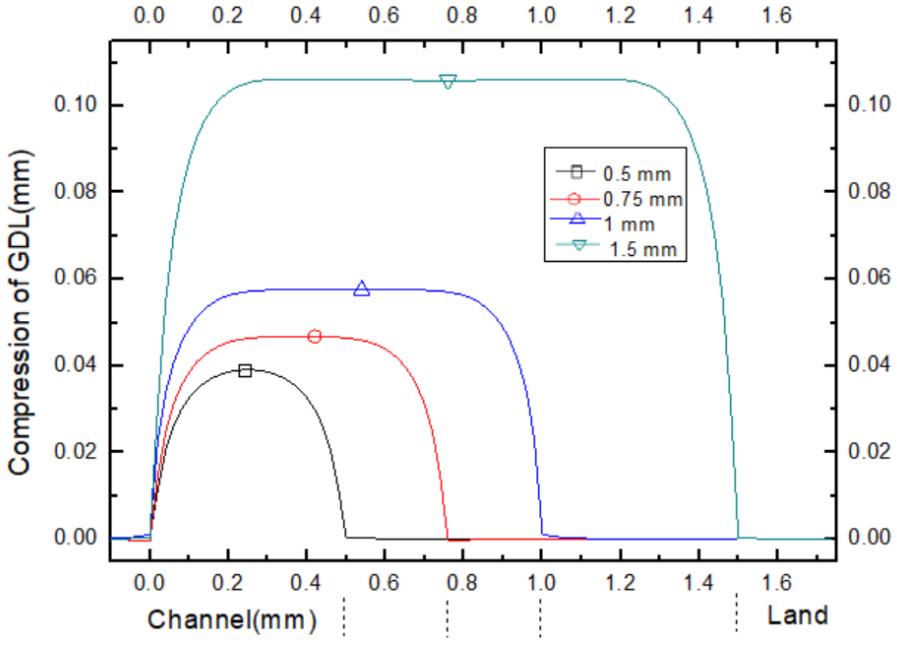


Figure 3.4. Deformation of GDL under the assembly pressures of 1 MPa

### 3.3 Effects of GDL height on intrusion of GDL

There is another factor which will affect the intrusion of GDL, that is height of GDL. The above simulation based on the height of GDL is 0.2 mm and the channel is hollow. Then the cases when the height of GDL is 0.3 also considered. Fig 3.5 a and b show the shapes of the compression of GDL when the height of GDL 0.2 mm and 0.3mm under different pressures, ranging from 0.5, 1, 1.5, 2 MPa. It shows that when the height of GDL increases, the intrusion of GDL will increase when the channel/land width ration is the same. For example, when the GDL is 0.2 mm, channel width is 2mm, the pressure is 1 MPa, the maximum of intrusion of GDL is 0.05749 mm. when the GDL is 0.3 mm, channel width is 2mm, the pressure is 1 MPa, the maximum of intrusion of GDL is 0.08314 mm, it increases 44.6%.

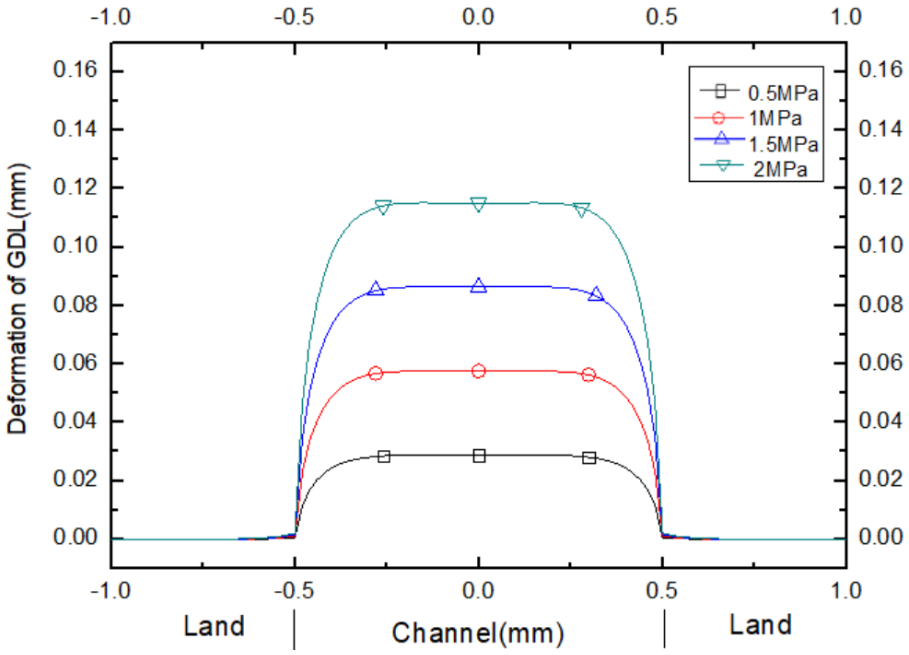


Figure 3.5a. Deformation of GDL for the GDL height of 0.2 mm

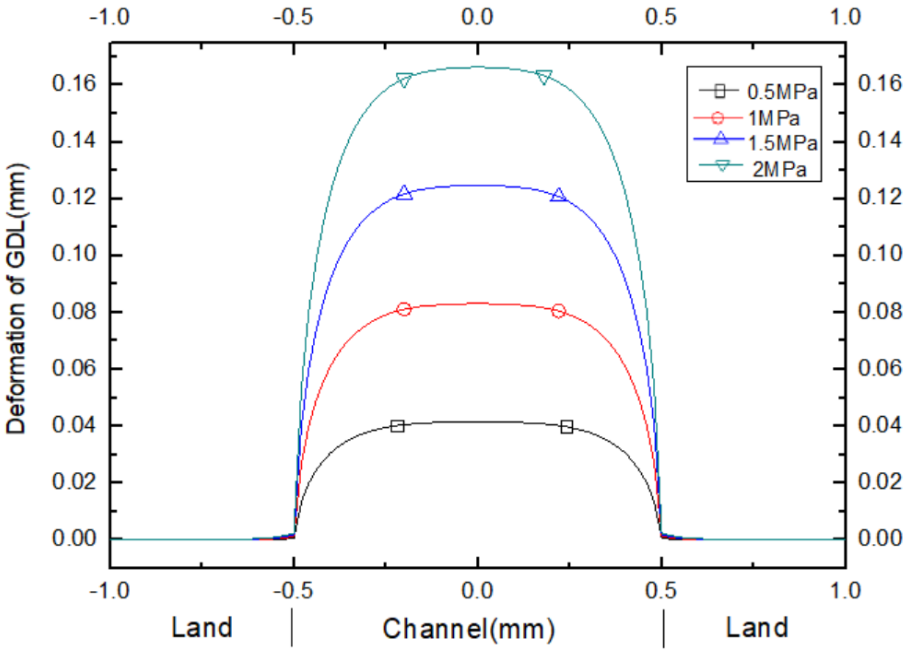


Figure 3.5b. Deformation of GDL for the GDL height of 0.3 mm

Figure 3.5. a and b are the shapes of GDL when the height of GDL 0.2 mm and 0.3mm under different pressures, that is 0.5 MPa, 1 MPa, 1.5 MPa, and 2 MPa.

### 3.4 Effects of porous media channel on intrusion of GDL

In this part, we consider three porous media with different Young's modulus, that is 1.26 MPa, 6.3 MPa, and 31.5 MPa. Figure 3.6 show that When the channel is full of porous media, the intrusion of GDL will decrease compare with the channel is hollow. Figure 3.6a is the deformation of GDL when the channel is hollow, the deformation is the same when the channel height is 0.3 mm with 0.6 mm. Figure 3.6b is the deformation of GDL when the channel is full of porous media. The intrusion of GDL decrease a lot. For example, under the same assembly pressure 1 MPa, the maximum of intrusion of GDL is 0.05749 mm with

hollow channel, however, the maximum of intrusion of GDL is 0.03815 mm with porous media channel. It decreases about 44.6%.

Figure 3.7 is the deformation of GDL when the channel is hollow, channel porous media Young's modulus. It shows that the intrusion of GDL decrease with the increasing of porous media's Young's modulus, and the maximum of intrusion occur when the channel is hollow. For example, when porous media Young's modulus is 1.26 MPa, the maximum of intrusion is 0.09782 mm, meanwhile, when porous media Young's modulus is 6.3 MPa, the maximum of intrusion is 0.06372 mm. it decreases about 34.9%.

In this research, we also study the effects of different channel height on the intrusion of GDL. We compare three types of channel height, 0.3 mm, 0.6 mm, 1 mm. Figure 7 shows that under the condition that the channel is full of porous media, the intrusion will increase with the increasing of channel height. When the channel height is 0.3 mm, the maximum of GDL intrusion is 0.05029 mm. When the channel height is 1 mm, the maximum of GDL intrusion is 0.06772 mm. figure the intrusion change ratio of GDL when the channel height change from 1 mm to 0.3 mm and 0.6 mm to 0.3 mm under the condition that the channel is full of porous. It shows that the maximum of change ratio is about 25.4%.

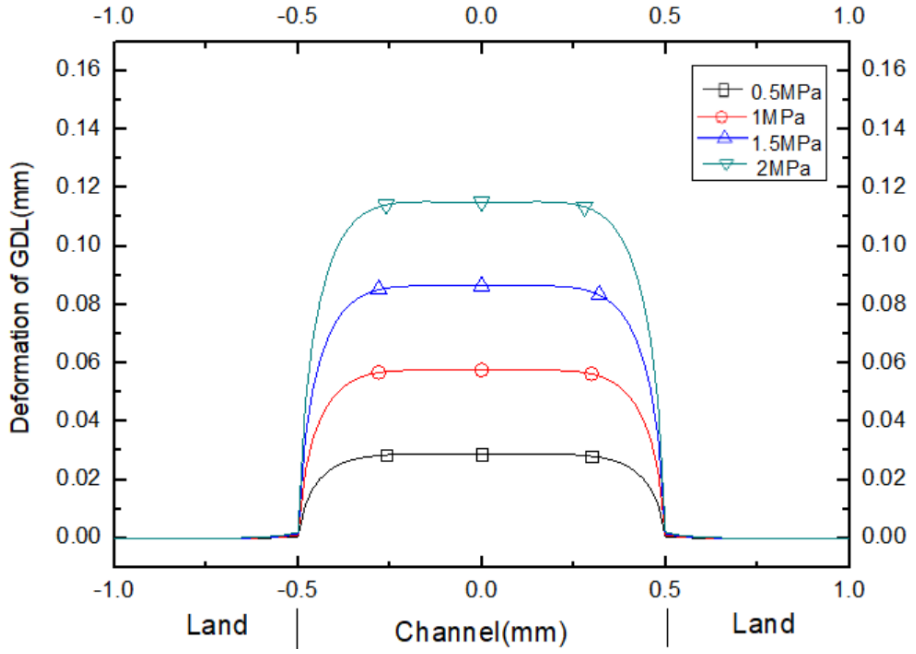


Figure 3.6a. Deformation of GDL for the hollow channel height of 0.3 mm

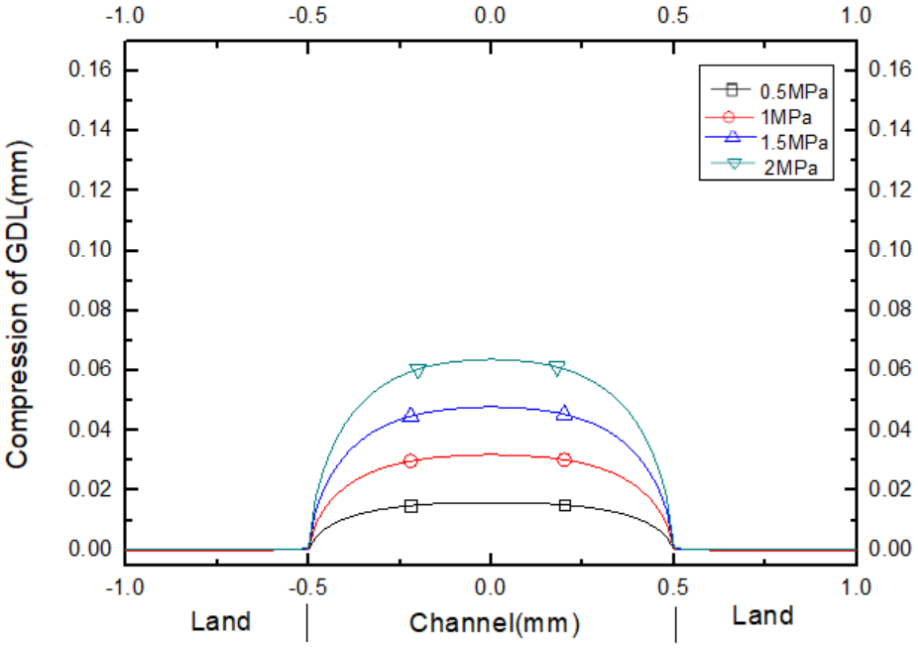


Figure 3.6b. Deformation of GDL for the porous media channel height of 0.3 mm

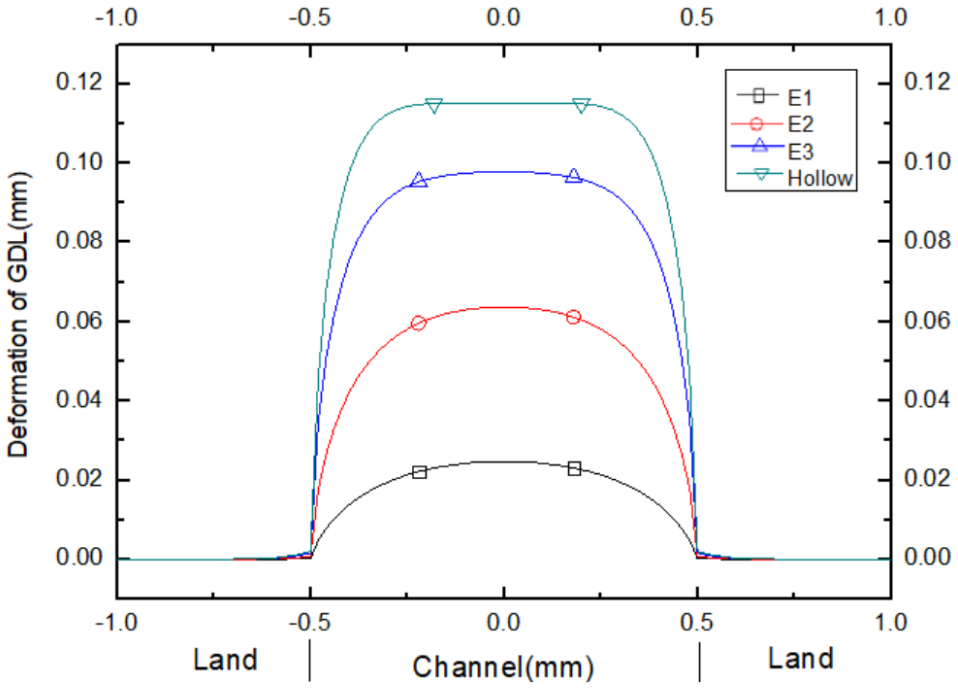


Figure 3.7. Deformation of GDL for porous media flow field with different Young's modulus

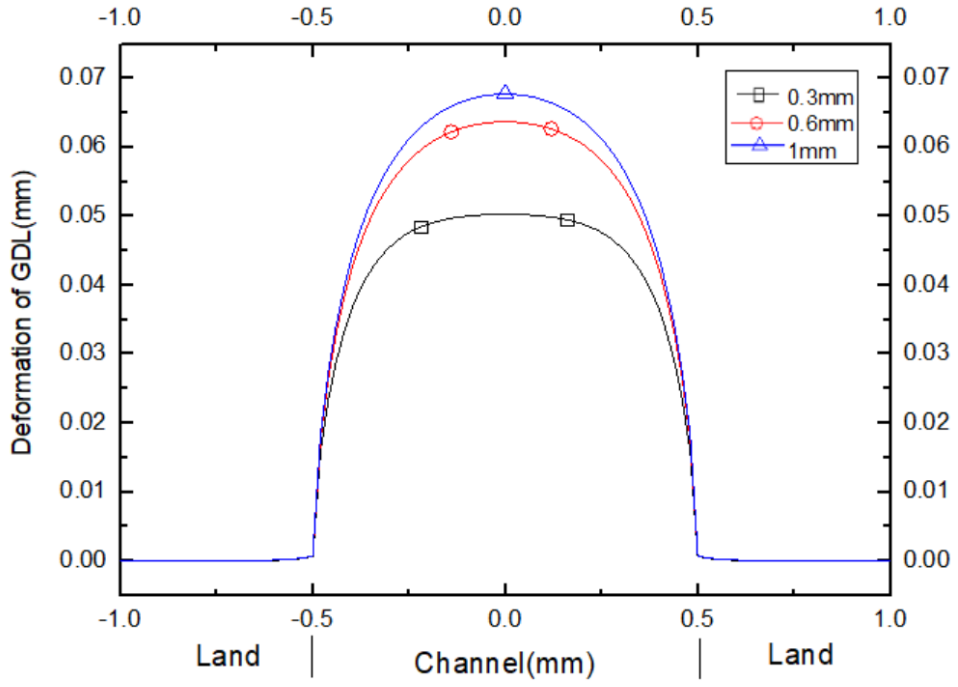


Figure 3.8. Deformation of GDL with different porous media channel heights

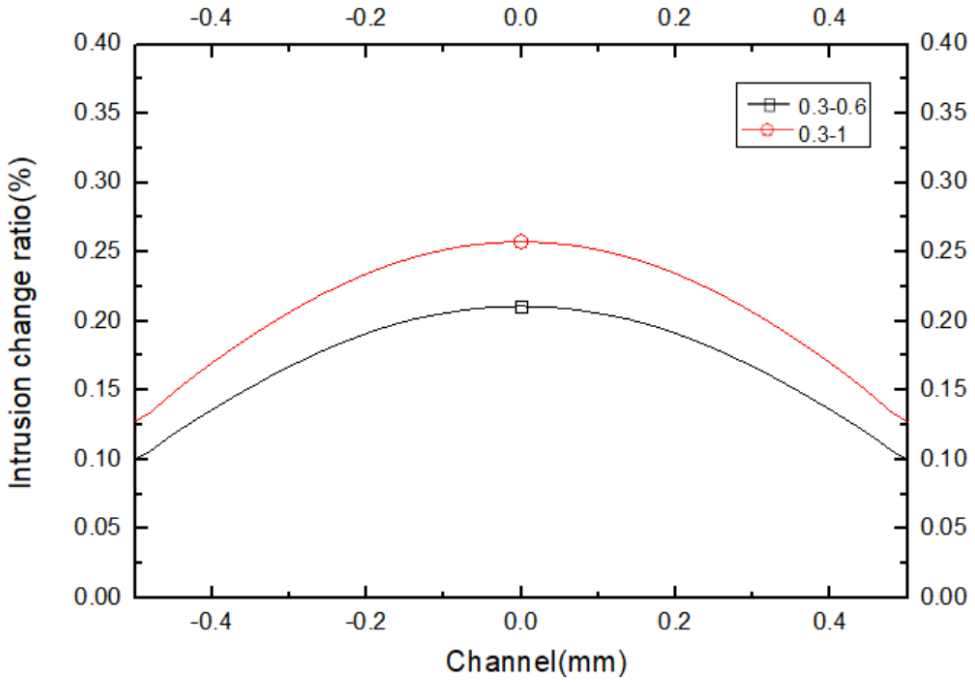


Figure 3.9. Deformation change ratio of GDL with different porous media channel heights

### 3.5 Effects of hollow channel on delamination between GDL and MPL

In most of the previous simulation research about GDL deformation in the literature, the MPL was excluded. In this study, the MPL is also considered for two conditions, one is a hollow channel, the other is a porous media channel. For the former case, Figure 3.10 shows that there is tensile stress in the middle of channel, which means GDL and MPL will separate and form a gap between them. And compare Figure 3.10a and Figure 3.10b, it is found that when the Young's modulus is higher, the tensile stress is less. For example, Figure 3.10a shows that when MPL's Young's modulus is 6.3 MPa and the assembly pressure is 1 MPa, the maximum of tensile stress is 0.01485 MPa. Figure 3.10b shows that when MPL's Young's modulus is 31.5 MPa and the assembly pressure is 1 MPa, the maximum of tensile stress is 0.01018 MPa.

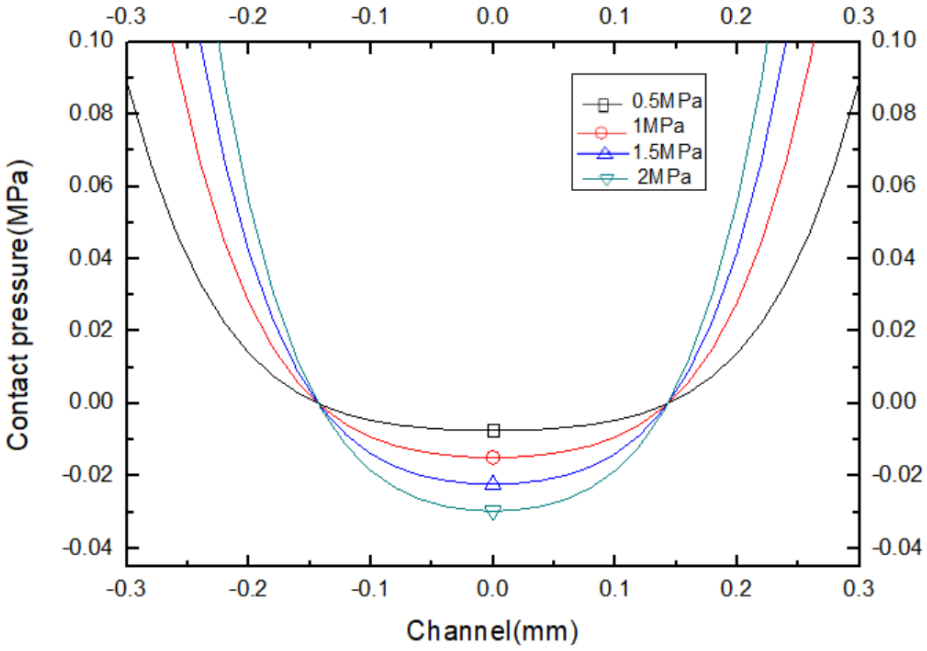


Figure 3.10a. Contact pressure between GDL and MPL with hollow channel, and the Young's modulus of MPL is 6.3 MPa

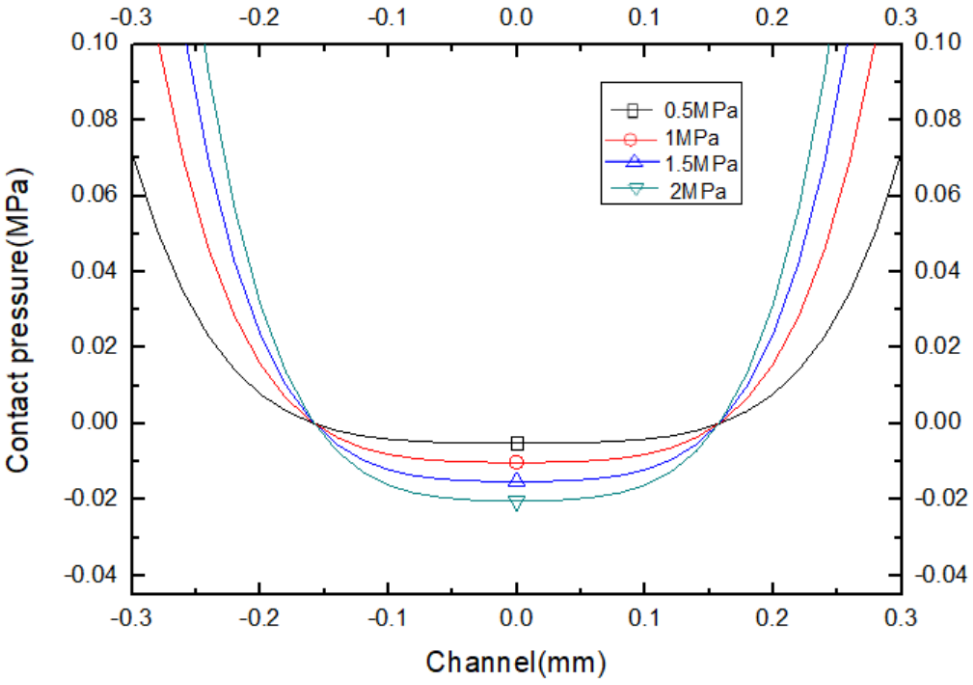


Figure 3.10b. Contact pressure between GDL and MPL with hollow channel, and the Young's modulus of MPL is 31.5 MPa

### 3.6 Effects of porous media channel on delamination between GDL and MPL

Two different Young's modulus of porous media were studied, one is 6.3 MPa, the other is 31.5 MPa. Figure 3.11 shows that when the channel is full of porous media, the force between the GDL and MPL is only compressive stress, which means there is no separate between them. It also shows that the compressive stress decrease with the increasing of Young's modulus of porous media. For example, Figure 3.11a shows that when the assembly pressure is 1 MPa and the Young's modulus of porous media is 6.3 MPa, the minimum of compressive stress between GDL and MPL is 0.59433 MPa. Figure 3.11b shows that when the assembly pressure is 1 MPa and the Young's modulus of porous media is 31.5 MPa, the minimum of compressive stress between GDL and MPL is 0.55541 MPa.

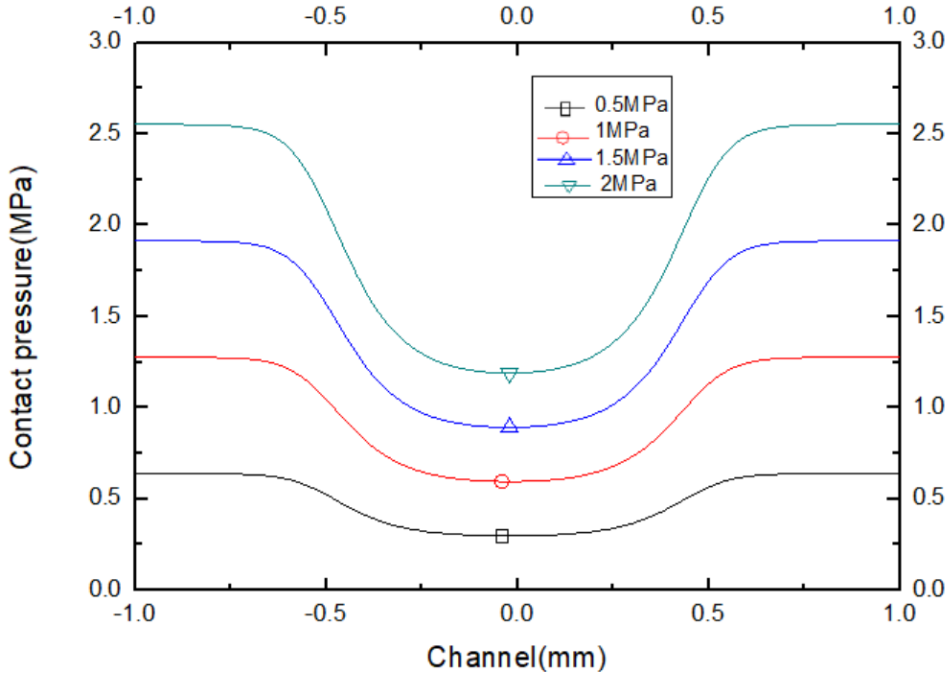


Figure 3.11a. Contact pressure between GDL and MPL with a porous media channel with the Young's modulus of MPL is 6.3 MPa

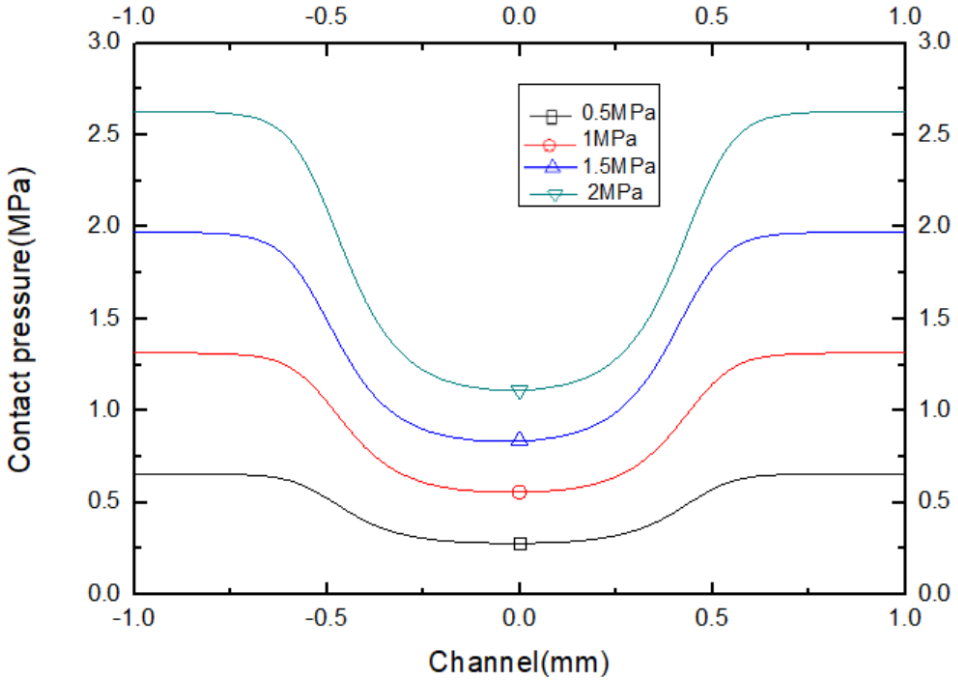


Figure 3.11b. Contact pressure between GDL and MPL with a porous media channel with the MPL Young's modulus 31.5 MPa

# Chapter.5 CONCLUSIONS

This research investigated the intrusion and delamination of GDL under different assembly pressures and channel configurations using a FEM model. It contains BP, GDL, MPL and porous media. The FEM model describes a three-dimensional domain composing of a single channel. Various GDL-channel configurations were investigated, including hollow and porous media, material properties, and dimensions. The predictions matched well with other studies and experiments. We found that:

1.) The intrusion of GDL into the channel increases with the increasing of assembly pressure. when the channel width is 1 mm, with the pressure change from 0.5 MPa to 2 MPa, the maximum of intrusion of GDL changes from 0.02874 mm to 0.11497 mm.

2.) When the channel is full of porous media, the intrusion of GDL will decrease compared with the case when the channel is hollow. Under the same1 MPa assembly pressure, the maximum of intrusion of GDL is 0.05749 mm with the hollow channel. However, the maximum of intrusion of GDL is 0.03815 mm with the porous media channel. It decreases by about 44.6%.

3.) The intrusion of GDL decreases with increasing of the Young's modulus of the porous media. When the Young's modulus porous media is 1.26 MPa, the maximum of intrusion is 0.09782 mm, meanwhile, when the Young's modulus of the porous media is 6.3 MPa, the maximum of intrusion is 0.06372 mm. It decreases by about 34.9%.

Since some company used a GDL of the 0.3mm thickness, we performed a simulation of it, and found that the intrusion is larger than the case when the GDL thickness is 0.2mm. In this view, the porous media helps to reduce the deformation of GDL.

To investigate the GDL delamination, we added the MPL and investigated the MPL-GDL internal force under compression. We found that when the channel is hollow, there is a tensile stress between GDL and MPL, which means they will separate when assembling the fuel cell. Porous media flow fields were also investigated to compare with traditional configuration to show the advantages of porous media flow field in depressing the intrusion and delamination. Major findings are listed below:

1.) When the channel is full of porous media, the force between the GDL and MPL is only compressive stress, which means there is no delamination between them.
2.) The compressive stress between GDL and MPL decrease with the increasing of Young's modulus of the porous media. When the assembly pressure is 1 MPa and the Young's modulus of the porous media is 6.3 MPa, the minimum of compressive stress between GDL and MPL is 0.59433 MPa. When the assembly pressure is 1 MPa and the Young's modulus of the porous media is 31.5 MPa, the minimum of compressive stress between GDL and MPL is 0.55541 MPa.

This study shows that the porous media flow field is benefit to depression of GDL intrusion into channels and the delamination between GDL and MPL. As a result, adoption of this new flow field approach will improve fuel cell performance and durability.

# Reference


[1]. Wang Y, Chen KS, Mishler J, Cho SC, Adroher XC. A review of polymer electrolyte membrane fuel cells: Technology, applications, and needs on fundamental research. Applied energy. 2011 Apr 1;88(4):981-1007.

[2]. Wang Y, Diaz DF, Chen KS, Wang Z, Adroher XC. Materials, technological status, and fundamentals of PEM fuel cells–a review. Materials Today. 2019 Jul 29. https://doi.org/10.1016/j.mattod.2019.06.005

[3]. Wang Y, Basu S, Wang CY. Modeling two-phase flow in PEM fuel cell channels. Journal of Power Sources. 2008 May 1;179(2):603-17.

[4]. Wang Y, Wang CY, Chen KS. Elucidating differences between carbon paper and carbon cloth in polymer electrolyte fuel cells. Electrochimica Acta. 2007 Mar 10;52(12):3965-75.

[5]. Wang X, Zhang H, Zhang J, Xu H, Zhu X, Chen J, Yi B. A bi-functional micro-porous layer with composite carbon black for PEM fuel cells. Journal of Power Sources. 2006 Nov 8;162(1):474-9.

[6]. Barbir F. PEM fuel cells: theory and practice. Academic Press; 2012 Oct 9.

[7]. Wang Y. Porous-media flow fields for polymer electrolyte fuel cells II. Analysis of channel two-phase flow. Journal of the Electrochemical Society. 2009 Oct 1;156(10): B1134-41.

[8]. Niu, Z., Wu, J., Wang, Y., & Jiao, K. (2018). Investigating the in-/through-plane effective diffusivities of dry and partially-saturated gas diffusion layers. Journal of The Electrochemical Society, 165(11), F986-F993.

[9]. Niu, Z., Wu, J., Bao, Z., Wang, Y., Yin, Y., & Jiao, K. (2019). Two-phase flow and oxygen transport in the perforated gas diffusion layer of proton exchange membrane fuel cell. International Journal of Heat and Mass Transfer, 139, 58-68.

[10]. Wang, Y., & Chen, K. S. (2016). Advanced control of liquid water region in diffusion media of polymer electrolyte fuel cells through a dimensionless number. Journal of Power Sources, 315, 224-235.

[11]. Cho, S. C., & Wang, Y. (2014). Two-phase flow dynamics in a micro hydrophilic channel: A theoretical and experimental study. International Journal of Heat and Mass Transfer, 70, 340-352.

[12]. Wang, Y., & Gundevia, M. (2013). Measurement of thermal conductivity and heat pipe effect in hydrophilic and hydrophobic carbon papers. International Journal of Heat and Mass Transfer, 60, 134-142.

[13]. Wu, J., Li, Y., & Wang, Y. (2019). Three-dimension simulation of two-phase flows in a thin gas flow channel of PEM fuel cell using a volume of fluid method. International Journal of Hydrogen Energy. https://doi.org/10.1016/j.ijhydene.2019.09.149

[14]. Lewis, J. M., & Wang, Y. (2019). Two-phase frictional pressure drop in a thin mixed-wettability microchannel. International Journal of Heat and Mass Transfer, 128, 649-667.

[15]. Lewis, J. M., & Wang, Y. (2018). Two-phase frictional pressure drop and water film thickness in a thin hydrophilic microchannel. International Journal of Heat and Mass Transfer, 127, 813-828.

[16]. Wang Y. Porous-media flow fields for polymer electrolyte fuel cells I. Low humidity operation. Journal of The Electrochemical Society. 2009 Oct 1;156(10): B1124-33.

[17]. Wang J, Yuan J, Yu JS, Sundén B. Investigation of effects of non‐homogenous deformation of gas diffusion layer in a PEM fuel cell. International Journal of Energy Research. 2017 Nov;41(14):2121-37.

[18]. Wang Y, Wang CY, Chen KS. Elucidating differences between carbon paper and carbon cloth in polymer electrolyte fuel cells. Electrochimica Acta. 2007 Mar 10;52(12):3965-75.

[19]. Tang Y, Kusoglu A, Karlsson AM, Santare MH, Cleghorn S, Johnson WB. Mechanical properties of a reinforced composite polymer electrolyte membrane and its simulated performance in PEM fuel cells. Journal of Power Sources. 2008 Jan 10;175(2):817-25.

[20]. Lai YH, Rapaport PA, Ji C, Kumar V. Channel intrusion of gas diffusion media and the effect on fuel cell performance. Journal of Power Sources. 2008 Sep 15;184(1):120-8.

[21]. Lai X, Peng L, Ni J. A mechanical–electrical finite element method model for predicting contact resistance between bipolar plate and gas diffusion layer in PEM fuel cells. Journal of Power Sources. 2008 Jul 15;182(1):153-9.

[22]. Bograchev D, Gueguen M, Grandidier JC, Martemianov S. Stress and plastic deformation of MEA in fuel cells: Stresses generated during cell assembly. Journal of Power Sources. 2008 May 15;180(1):393-401.

[23]. Lee SJ, Hsu CD, Huang CH. Analyses of the fuel cell stack assembly pressure. Journal of power sources. 2005 Aug 18;145(2):353-61.

[24]. Taymaz I, Benli M. Numerical study of assembly pressure effect on the performance of proton exchange membrane fuel cell. Energy. 2010 May 1;35(5):2134-40.

[25]. Chippar P, Kyeongmin O, Kang K, Ju H. A numerical investigation of the effects of GDL compression and intrusion in polymer electrolyte fuel cells (PEFCs). international journal of hydrogen energy. 2012 Apr 1;37(7):6326-38.

[26]. Bates A, Mukherjee S, Hwang S, Lee SC, Kwon O, Choi GH, Park S. Simulation and experimental analysis of the clamping pressure distribution in a PEM fuel cell stack. International journal of hydrogen energy. 2013 May 20;38(15):6481-93.

[27]. Tötzke C, Gaiselmann G, Osenberg M, Bohner J, Arlt T, Markötter H, Hilger A, Wieder F, Kupsch A, Müller BR, Hentschel MP. Three-dimensional study of compressed gas diffusion layers using synchrotron X-ray imaging. Journal of Power Sources. 2014 May 1;253:123-31.

[28]. Zhou Y, Lin G, Shih AJ, Hu SJ. A micro-scale model for predicting contact resistance between bipolar plate and gas diffusion layer in PEM fuel cells. Journal of Power Sources. 2007 Jan 1;163(2):777-83.

[29]. Zhou X, Niu Z, Bao Z, Wang J, Liu Z, Yin Y, Du Q, Jiao K. Two-phase flow in compressed gas diffusion layer: Finite element and volume of fluid modeling. Journal of Power Sources. 2019 Oct 15;437: 226933.

[30]. Zhou Y, Lin G, Shih AJ, Hu SJ. Assembly pressure and membrane swelling in PEM fuel cells. Journal of Power Sources. 2009 Jul 15;192(2):544-51.

[31]. Zhou Y, Jiao K, Du Q, Yin Y, Li X. Gas diffusion layer deformation and its effect on the transport characteristics and performance of proton exchange membrane fuel cell. International Journal of Hydrogen Energy. 2013 Sep 30;38(29):12891-903.

[32]. Lee WK, Ho CH, Van Zee JW, Murthy M. The effects of compression and gas diffusion layers on the performance of a PEM fuel cell. Journal of power sources. 1999 Nov 1;84(1):45-51.

[33]. Ge J, Higier A, Liu H. Effect of gas diffusion layer compression on PEM fuel cell performance. Journal of Power Sources. 2006 Sep 22;159(2):922-7.

[34]. Kandlikar SG, Lu Z, Lin TY, Cooke D, Daino M. Uneven gas diffusion layer intrusion in gas channel arrays of proton exchange membrane fuel cell and its effects on flow distribution. Journal of Power Sources. 2009 Oct 20;194(1):328-37.

[35]. Baik KD, Hong BK, Han K, Kim MS. Correlation between anisotropic bending stiffness of GDL and land/channel width ratio of polymer electrolyte membrane fuel cells. international journal of hydrogen energy. 2012 Aug 1;37(16):11921-33.

[36]. Chang WR, Hwang JJ, Weng FB, Chan SH. Effect of clamping pressure on the performance of a PEM fuel cell. Journal of Power Sources. 2007 Mar 30;166(1):149-54.

[37]. Nitta I, Hottinen T, Himanen O, Mikkola M. Inhomogeneous compression of PEMFC gas diffusion layer: part I. Experimental. J. Power Sources. 2007 Sep 19;171(1):26-36.

[38]. Zhang FY, Advani SG, Prasad AK. Performance of a metallic gas diffusion layer for PEM fuel cells. Journal of power sources. 2008 Jan 21;176(1):293-8.

[39]. Nguyen TV, Lin G, Ohn H, Hussey D, Jacobson D, Arif M. Measurements of two-phase flow properties of the porous media used in PEM fuel cells. ECS transactions. 2006 Oct 20;3(1):415-23.

[40]. Siegkas P, Tagarielli VL, Petrinic N, Lefebvre LP. The compressive response of a titanium foam at low and high strain rates. Journal of Materials Science. 2011 Apr 1;46(8):2741-7.

[41]. Kim S, Khandelwal M, Chacko C, Mench MM. Investigation of the impact of interfacial delamination on polymer electrolyte fuel cell performance. Journal of the Electrochemical Society. 2009 Jan 1;156(1): B99-108.

[42]. Kim S, Ahn BK, Mench MM. Physical degradation of membrane electrode assemblies undergoing freeze/thaw cycling: Diffusion media effects. Journal of Power Sources. 2008 Apr 15;179(1):140-6.

[43]. Zhou X, Niu Z, Li Y, Sun X, Du Q, Xuan J, Jiao K. Investigation of two-phase flow in the compressed gas diffusion layer microstructures. International Journal of Hydrogen Energy. 2019 Oct 8;44(48):26498-516.

[44]. Pich PK. Investigation of catalysts, diffusors, and collector plates and their effects on PEM fuel cell performance. The University of Texas at El Paso; 2004.

[45]. Park S, Popov BN. Effect of a GDL based on carbon paper or carbon cloth on PEM fuel cell performance. Fuel. 2011 Jan 1;90(1):436-40.